Integration of inter-ply electrical percolation phenomena in the multiphysics modelling of laminated composite materials

Banda Kane, Guillaume Wasselynck, Didier Trichet, Gerard Berthiau

Integration of inter-ply electrical percolation phenomena in the multiphysics modelling of laminated composite materials

Banda KANE, Guillaume WASSELYNCK, Didier TRICHET, and Gérard BERTHIAU

Nantes University, Institute for Research in Electrical Energy of Nantes-Atlantique, IREENA, UR 4642,
37 Boulevard de l'Université, CS 90406, F-44600 Saint-Nazaire, France

ABSTRACT

Purpose - This study aims to introduce a predictive homogenization model incorporating electrical percolation considerations to forecast the electrical characteristics of unidirectional carbon-epoxy laminate composites.

Design/methodology/approach - We present a method for calculating the electrical conductivity tensor for various ply arrangement patterns to elucidate phenomena occurring around the interfaces between plies. These interface models are then integrated into a three-dimensional magneto-thermal model using the finite element method (FEM). A comparative study is conducted between different approaches, emphasizing the advantages of the new model through experimental measurements.

Findings - This research facilitates the innovative integration of electrical percolation considerations, resulting in substantial improvement in the prediction of electrical properties of composites. The validity of this improvement is established through comprehensive validation against existing approaches and experimentation.

Research limitations/implications - The study primarily focuses on unidirectional carbon-epoxy laminate composites. Further research is needed to extend the model's applicability to other composite materials and configurations.

Originality/value - The proposed model offers a significant improvement in predicting the electrical properties of composite materials by incorporating electrical percolation considerations at inter-ply interfaces, which have not been addressed in previous studies. This research provides valuable information to improve the accuracy of predictions of the electrical properties of composites and offers a methodology for accounting for these properties in 3D magneto-thermal simulations.

Keywords - Anisotropy, Electrical characterization, Electrical percolation, Homogenization model, Phenomena of interface, Stratified composite material, Virtual materials.

Paper type - Research paper

I. INTRODUCTION

Composite materials have transformed material design by enabling their mechanical properties to adapt to specific shapes and stresses. Carbon Fiber-Reinforced Polymer (CFRP) laminate composites are particularly useful in the aeronautics and space industries because of their ability to meet strict weight and space requirements. However, unlike homogeneous metal structures, CFRP composites have strong anisotropic electrical conductivity due to the alignment of conductive carbon fibers within each ply, as shown in Fig. 1. A CFRP laminate composite is a stack of multiple plies, with adjacent plies potentially having different fiber orientations to optimize mechanical performance (Meltem Altin Karataş, 2018).

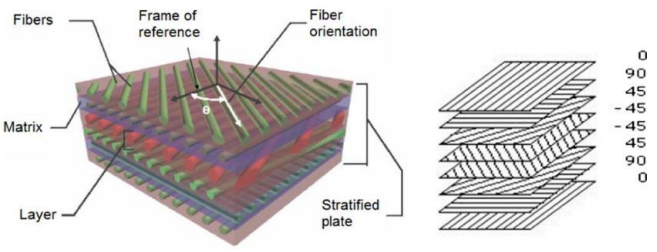

Fig. 1. (a) CFRP, (b) Fiber orientation (Wasselynck, et al., 2013). Source: figure created by author (Guillaume Wasselynck)

Composite materials require heat input for various processes such as polymerization, forming, welding, and recycling. Electromagnetic induction is a promising heating method for these materials because of the high electrical conductivity of carbon fibers, which offers a faster cycle time and no contact between the source coil and the load (Ahmed, et al., 2006) (Buckley JD, 1988).

The 3D computational codes in the A-φ formulation developed in (Wasselynck, et al., 2010) were employed for electromagnetic simulations of composites.

$$\begin{cases} curl\left(\frac{1}{\mu} curl\boldsymbol{A}\right) + [\boldsymbol{\sigma}](grad\varphi + j\omega\boldsymbol{A}) = \boldsymbol{J_0} = curl(\boldsymbol{H_0}) \\ div(\boldsymbol{J}) = div([\boldsymbol{\sigma}](grad\varphi + j\omega\boldsymbol{A})) = 0 \end{cases} \quad (1)$$

where μ is the permeability, ω is the field pulsation, $\boldsymbol{H_0}$ is the source magnetic field, and $\boldsymbol{J}$ is the current density.

The equation highlights the importance of accurately determining of the conductivity tensor $[\boldsymbol{\sigma}]$ for the effective evaluation of the location of the electromagnetic power and for good control of the heating process (Qian, et al., 2019). Thus, a numerical model that allows the careful determination of the conductivity tensor is necessary. Owing to the important scale factor between the fiber diameter and composite dimensions, a transition from microscopic to mesoscopic scale will be necessary to account for the phenomena with reasonable numerical complexity. A multi-scale predictive homogenization method, addressing

percolation, was proposed in (Wasselynck, et al., 2010), (Wasselynck, et al., 2013) and (Kane, et al., 2019) to overcome this constraint. In this approach, the composite is divided ply by ply, and the electrical tensor of each ply is determined.

Within each ply, undulating fibers established electrical contacts between adjacent fibers, facilitating current passage through percolation in all ply directions (Park, et al., 2007). To address this complexity, the ply was subdivided into several Representative Elementary Volumes (REVs) using a virtual-material homogenization procedure (Kane, et al., 2019). The previous work detailed in (Wasselynck, et al., 2010), (Wasselynck, et al., 2013) and (Kane, et al., 2019) provides comprehensive insights into the generation of 3D REVs with fibers oriented in the same direction. The electrical conductivity tensor was exclusively calculated for one ply. The tensor for other ply directions was then deduced through mathematical rotation (Wasselynck, et al., 2013). These transformations influence only the conductivities in the fiber direction and the transverse direction, without affecting the conductivity in the thickness direction.

To validate this hypothesis, experimental characterizations were conducted using the volt-amperometric method with a composite test bench presented in (Kane, et al., 2019). The electrical conductivities along the three directions for each specimen are listed in Table I. $\sigma_{\parallel}$ represents the electrical conductivity of the composite in the fiber direction, $\sigma_{\perp}$ is the transverse conductivity, and σ_z is the conductivity in the thickness direction. Specimens 1 and 2 consist of 7 unidirectional plies, all oriented at 0°. Specimen 3 comprises 7 unidirectional plies alternatively oriented at 0 and 90°. Each sample has a width x length of 40x40 mm with a thickness of 1.3 mm and a fiber filling rate of 60%.

TABLE I
CONDUCTIVITY MEASUREMENTS

Specimen	Sequence	Conductivity (S/m)		
		$\sigma_{\parallel}$	$\sigma_{\perp}$	σ_z
1	$(0)_7$	32732 S/m	8.51 S/m	2.07 S/m
2	$(0)_7$	32287 S/m	7.28 S/m	1.73 S/m
3	$[0/90]_3/0$	14744 S/m	14744 S/m	5.02 S/m

Source: Authors' own work

Although samples 1 and 2 are similar, they exhibit slight differences in their electrical conductivities owing to the different random positioning of the fibers from one sample to the other during the elaboration process. Moreover, a highly anisotropic ratio between $\sigma_{\parallel}$ and $\sigma_{\perp}$ is evident. The conductivity along the thickness is four times lower than the transverse conductivity. Measurements carried out by Todoroki et al in (Todoroki, et al., 2002) on other types of samples showed a conductivity along the thickness ten times greater than the transverse conductivity, which is attributed to phenomena at the ply interfaces. Lastly, specimen 3 demonstrates that these phenomena depend on the sequence of ply orientations.

Evidently, conductivity along the thickness is affected by the sequence of plies. To consider these phenomena, the existing model must be improved.

In this paper, we will highlight these phenomena using virtual generation of the area between two adjacent plies with different relative orientations. We will then show how to incorporate these phenomena into our 3D simulations in order to observe their influence on the thermal behavior of the simulated materials.

II. HOMOGENIZATION METHOD

The methodology employed in this study was based on the Representative Equivalent Volume (REV) generation approach described in (Wasselynck, et al., 2013). Relevant parameters are involved in the creation of 3D REV cells. These include the dimensions of the REV cell (width x, thickness z, and length y, denoted by nz as the number of slices), the spacing between slices (dz), which represents the frequency of potential contacts between fibers, and the volume filling rate (τ), all these parameters can be controlled. These parameters were studied and defined in (Kane, et al., 2019), providing a comprehensive understanding. Multiple REVs with robust statistical representation are consequently generated, and these REVs are assembled to achieve the desired width for larger unidirectional (UD) plies, as illustrated in Fig. 2.

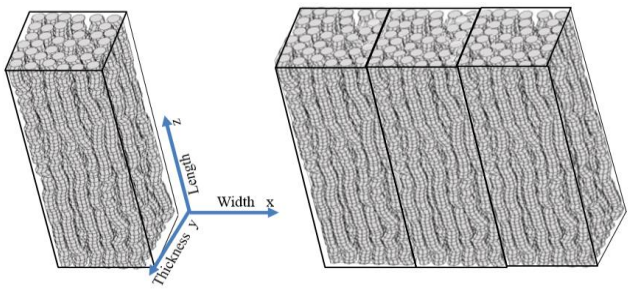

Fig. 2. REV assembly for a desired width
Source: Authors' own creation

With this methodology, a database of two types (named A and B) of UD plies of different sizes is established. These two types of plies, both with a thickness of 185µm, have different widths and lengths. Type A plies are 4.5x4.5mm, while type B plies are 6.5x6.5mm. The electrical properties calculated with these generated plies are as follows: $\sigma_{\parallel} = 34800$ S/m, $\sigma_{\perp} = 7.75 \pm 0.25\ S/m$ and $\sigma_z = 8.70 \pm 0.25\ S/m$.

To investigate the impact of the relative angle between two plies on conductivity through the thickness, one type A ply oriented at 0° and another of type B oriented at the desired angle are used. For connecting the two plies, contacts are detected at the interface of the two plies, as described in the algorithm in Fig. 3. A top view of the results obtained after stacking these two plies at an angle of 45° is shown in Fig. 4(a). The Type B ply (colored in green) completely covers that of Type A (colored blue) but extends beyond the limits of the latter. An operation is then necessary to remove excess volumes. In this operation, the desired size is defined (size of the Type A ply), and the shaping process is carried out, eliminating points outside the specified range while creating points along the edges of the study area for fibers that exceed. The geometry depicted in Fig. 4(b) is obtained after this operation. This procedure is generalized for the superposition of more than two plies.

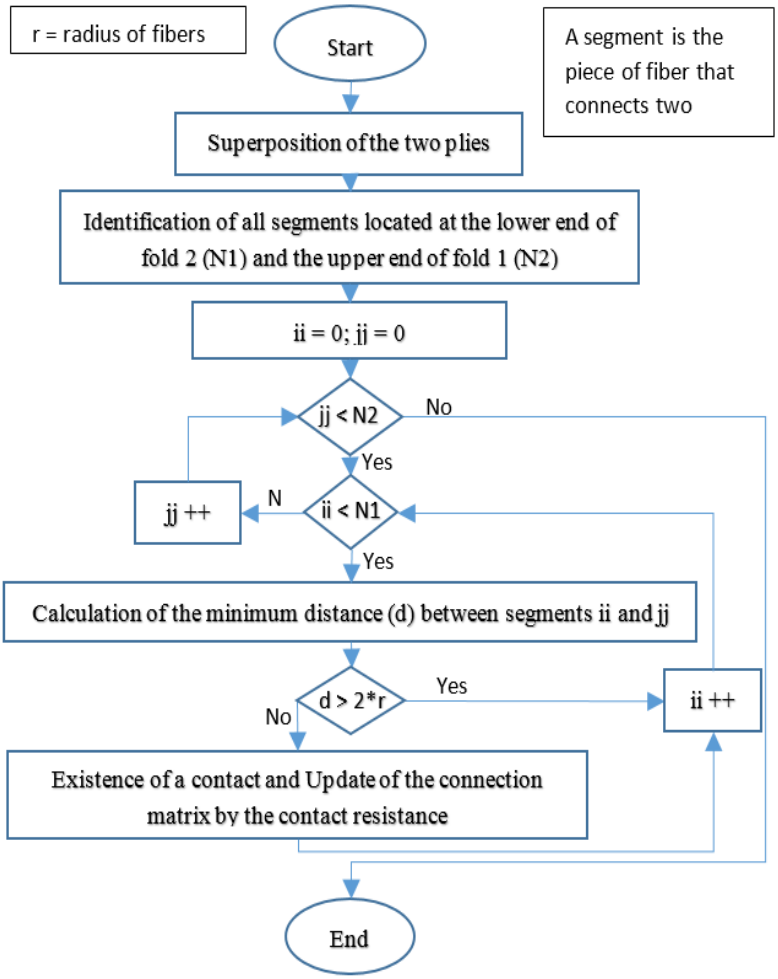

Fig. 3. Search for contacts at the interface of two plies
Source: Authors' own work

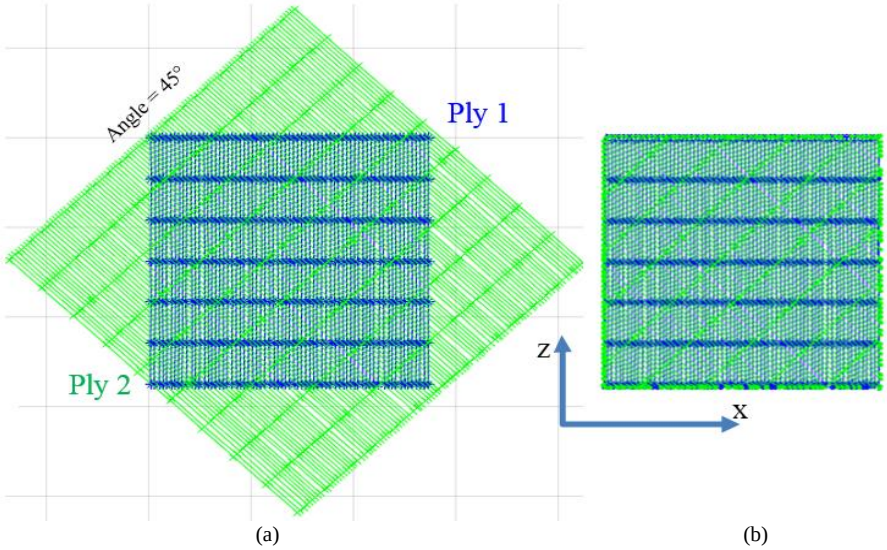

Fig. 4. Top view of the superposition of two plies
Source: Authors' own creation

Contact resistance at the two-ply interface

In the generation of virtual materials, we used the algorithm described in section II of (Kane, et al., 2019), which allows for an overlap between adjacent fibers measured in micrometers (µm). The overlap between two virtual fibers represents the depth to which the first fiber penetrates the second, as illustrated in the 2D view of figure 5 of (Kane, et al., 2019). Although this phenomenon is impossible in reality, it represents the strength of the global contact between two fibers. This consideration, along with the maximum allowed overlap, has been validated by the results obtained in (Kane, et al., 2019), (Wasselynck, et al., 2013) and (Wasselynck, et al., 2010).

To evaluate the contact resistance between two fibers at the interface of two plies, we developed a 3D electrokinetic model. This model takes into account the electrical characteristics of the fibers, the orientation angle between them, as well as the previously defined and measured overlap in micrometers (µm).

For each angle, using the 3D GMSH mesh shown in Fig. 5 (for 45°), the electrokinetic problem of equations 2 and 3 is solved by finite elements for different overlap values. This allows us to plot in Fig. 6 the curve of contact resistance as a function of overlap for angles 45 and 90°. The evaluation of this resistance for two fibers aligned in the same direction (angle of 0°) was discussed in (Kane, et al., 2019).

$$div(J) = div(\sigma E) = div\big(\sigma grad(V)\big) = 0 \tag{2}$$

$$\int_{\Omega} \overrightarrow{grad}(V)[\sigma](w)d\Omega - \int_{\Gamma} \frac{\partial V}{\partial n} w d\Gamma = 0 \tag{3}$$

Here, V represents the electrical potential, $[\sigma]$ the electrical conductivity of fibers and w the shape function.

Having established the various contact resistances, the next step involves interconnecting the electrical circuits of the two plies, resulting in the final resistance network. Subsequently, a volt-amperometric test is then conducted to obtain the conductivity tensor in all directions as illustrated in Fig. 7.

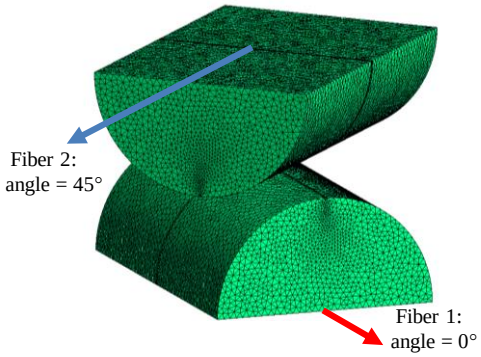

Fig. 5. 3D modeling of the contact between two fibers
Source: Authors' own creation

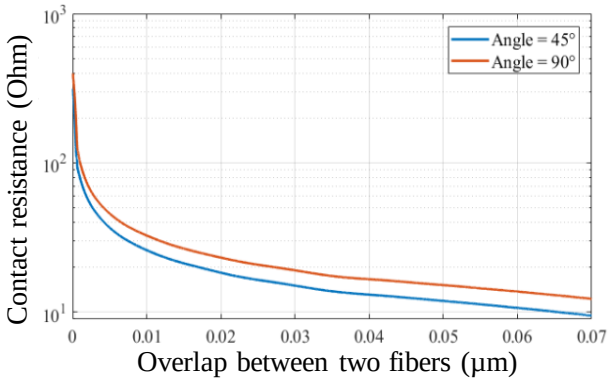

Fig. 6. Contact resistance as a function of overlap and orientation angle
Source: Authors' own work

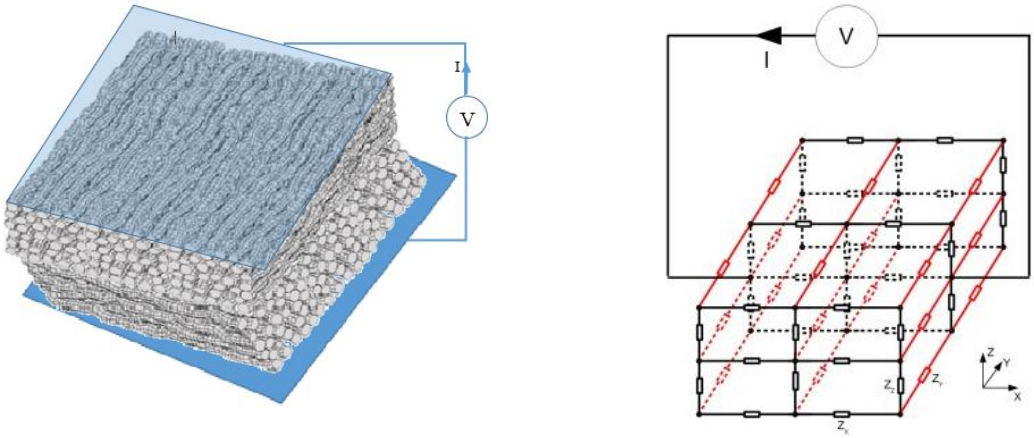

(a) (b)

Fig. 7. Network of impedances
Source: Authors' own creation

III. RESULTS

The electrical conductivity tensors simulated for specimens composed of a type A ply superimposed on another of type B for various angles are analyzed.

In Fig. 8(a), the variation of electrical conductivities in the direction of the fibers and in the transverse direction is presented as a function of the relative angle. The transverse electrical conductivity remains low for angles less than 45° but sharply increases from 45° to 90°, reaching its maximum at the latter angle. The curves exhibit symmetry with respect to 90°. Beyond 45°, some fibers in the upper ply may align with the transverse direction, establishing a highly conductive path for electrical current.

Similarly, the electrical conductivity in the fiber direction peaks at 0° but decreases with increasing angle up to 45°, after which it stabilizes. The two curves coincide at 90°, indicating that the REV configuration remains constant in both directions at this angle.

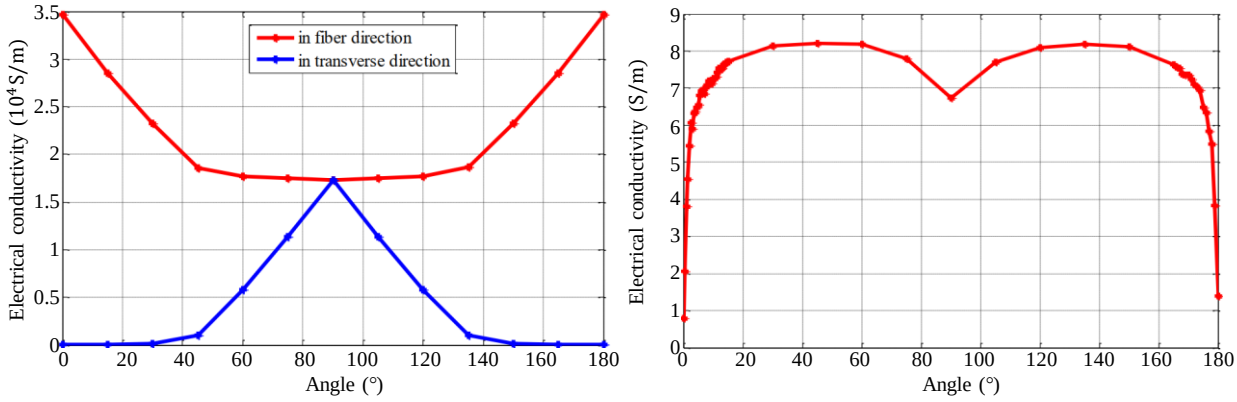

(a) (b)

Fig. 8. Electrical conductivities as a function relative angle (a) - in direction of the fibers and in the transverse direction; (b) - in the direction normal to the plies
Source: Authors' own work

Figure 8(b) illustrates the variation of electrical conductivity along the thickness direction of the plies for different angles. The electrical conductivity increases rapidly from 0 to 7° and then experiences slight variations. It decreases at 90° but appears to reach its maximum value at 45°. The heightened conductivity for angles greater than 7° can be attributed to increased electrical contacts between the two plies.

To validate the homogenization approach, conductivity measurements in the thickness direction were conducted for various samples of stratified composite materials using the test bench presented in (Kane, et al., 2019). Subsequently, the same sequence of plies was simulated using the model developed in this paper.

The results obtained in both cases are summarized in Table II. While a slight difference exists between the measured and simulated values, the agreement is notably improved compared to previous work, attesting to the effectiveness of the present homogenization procedure.

TABLE II
CONDUCTIVITY MEASUREMENTS IN THE THICKNESS DIRECTION

Sample	Sequence	Conductivity (S/m) Measured	Simulated
1	$(0)_7$	1.68 ± 0.06	1.46 ± 0.048
2	[45/135/0/90/90/0/ 90/90/0/135/45]	3.16 ± 0.14	4.33 ± 0.09
3	[45/135/0/0/0/90/90/135/45/0/45/135/90/90/0/0/0/135/45]	2.56 ± 0.04	3.01 ± 0.067

Source: Authors' own work

IV. VALIDATION

To investigate the impact of the interface phenomena between plies in stratified composite materials, a 3D simulation of the laminate composites was conducted. Initially, the simulation used the electrical conductivity tensor calculated without considering the interface phenomena (Wasselynck, et al., 2013). Subsequently, the simulation is repeated using the tensor determined in this study.

The heating problem is resolved utilizing a 3D anisotropic finite element method, incorporating distinct thermal conductivities along the three axes of the composite. This is achieved by solving equation (3) with the Fourier boundary condition defined in equation (4) (Jaluria & Torrance, 2003).

$$\rho C_p \frac{\partial T}{\partial t} + div\left(-[\lambda] grad(T)\right) = P \tag{3}$$

$$-[\lambda]\frac{\partial T}{\partial n} = h(T - T_a) \tag{4}$$

Here, C_p represents the specific heat, ρ is the mass density, λ is the thermal conductivity tensor, h is the convection coefficient, T is the temperature in the CFRP plate, T_a is the ambient temperature, and P is the induced power density obtained after solving the electromagnetic problem outlined in equation (1).

For simulations involving interface phenomena, an additional challenge arises in integrating the electrical conductivity tensor into the 3D model. The conductivity when considering the thickness of an individual ply, differs from the composite conductivity obtained when two plies are superimposed, as discussed earlier. To address this, we defined zones at the interface between the two plies, as illustrated in Fig. 9. In these zones, we established the electrical conductivity based on the thickness of the plies, ensuring that the equivalent conductivity of the stacked plies (considering the draping angle) corresponds to the values outlined in Table II. If we assume uniform thickness and conductivity in these zones for each ply, we derive the

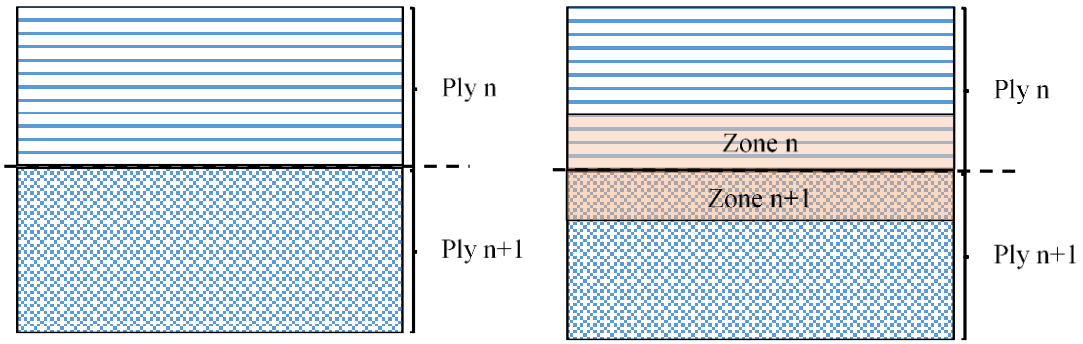

(a) With tensor in previous model (b) With tensor in section II

Fig. 9. Delimitation of interface areas
Source: Authors' own creation

relationship given by equation (5), where y represents the thickness of a ply, e is the thickness of a zone, and σ_i is the electrical conductivity in the interface zones.

$$y = \sigma_z \left(\frac{y-e}{\sigma_\perp} + \frac{e}{\sigma_i}\right) \tag{5}$$

This equation involves two unknowns, e and σ_i, which need to be determined. To achieve this, a sensitivity study is conducted to examine the impact of the zone thickness on the 3D results. The 11-ply composite (300x300x02mm) is subjected to heating by a U-shaped inductor (100x20x150 mm) with a current of 250 A at a frequency of 240 kHz. The air gap between the coil and the load is set at 2 mm.

By varying the thickness of the zone from a third of the ply thickness (y/3) to a tenth (y/10), the error in induced power in each ply is obtained, as presented in Fig. 10, with y/5 serving as the reference thickness of the zone. The results indicate that the induced power error does not exceed 2%, and the temperature error remains below 3% for a heating temperature of 400°C. Thus, it can be inferred that the thickness of the interface zone exerts a negligible influence, mainly contributing to meshing errors in simulation results.

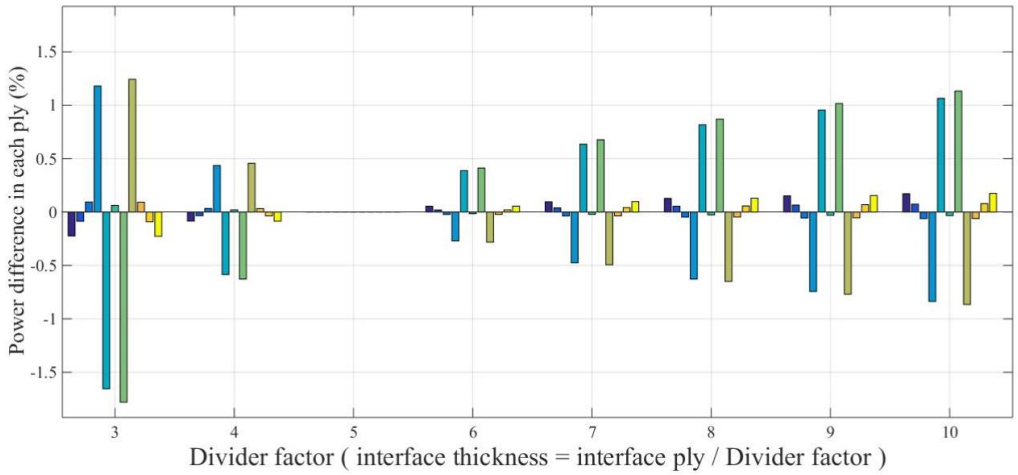

Fig. 10. Study of sensitivity
Source: Authors' own work

Model comparison

To assess the impact of incorporating interface phenomena in 3D simulations, a 14-ply unidirectional composite (300x300x2.6mm) was examined using the same U-shaped inductor as previously, supplied with a current of 131A at a frequency of 1.6 MHz, and an air gap of 2 mm between the coil and the load. This system was simulated with the 3D magnetothermal model, integrating the conductivity tensor calculated in previous work (Wasselynck, et al., 2013) (without considering interface phenomena) and then with the tensor determined in this article. An experimental test was also conducted on the same composite, measuring a temperature rise of 25°C compared to ambient temperature after 30 seconds of heating.

The temperature maps obtained from a bottom view in each case are shown in Fig. 11, revealing that the new model aligns more closely with the experimental results than the previous model. An analysis of the discrepancies between the two models exposes variations in induced power in specific areas of the composite, reaching up to 40%, along with temperature differences exceeding 65%, as illustrated in Figure 12.

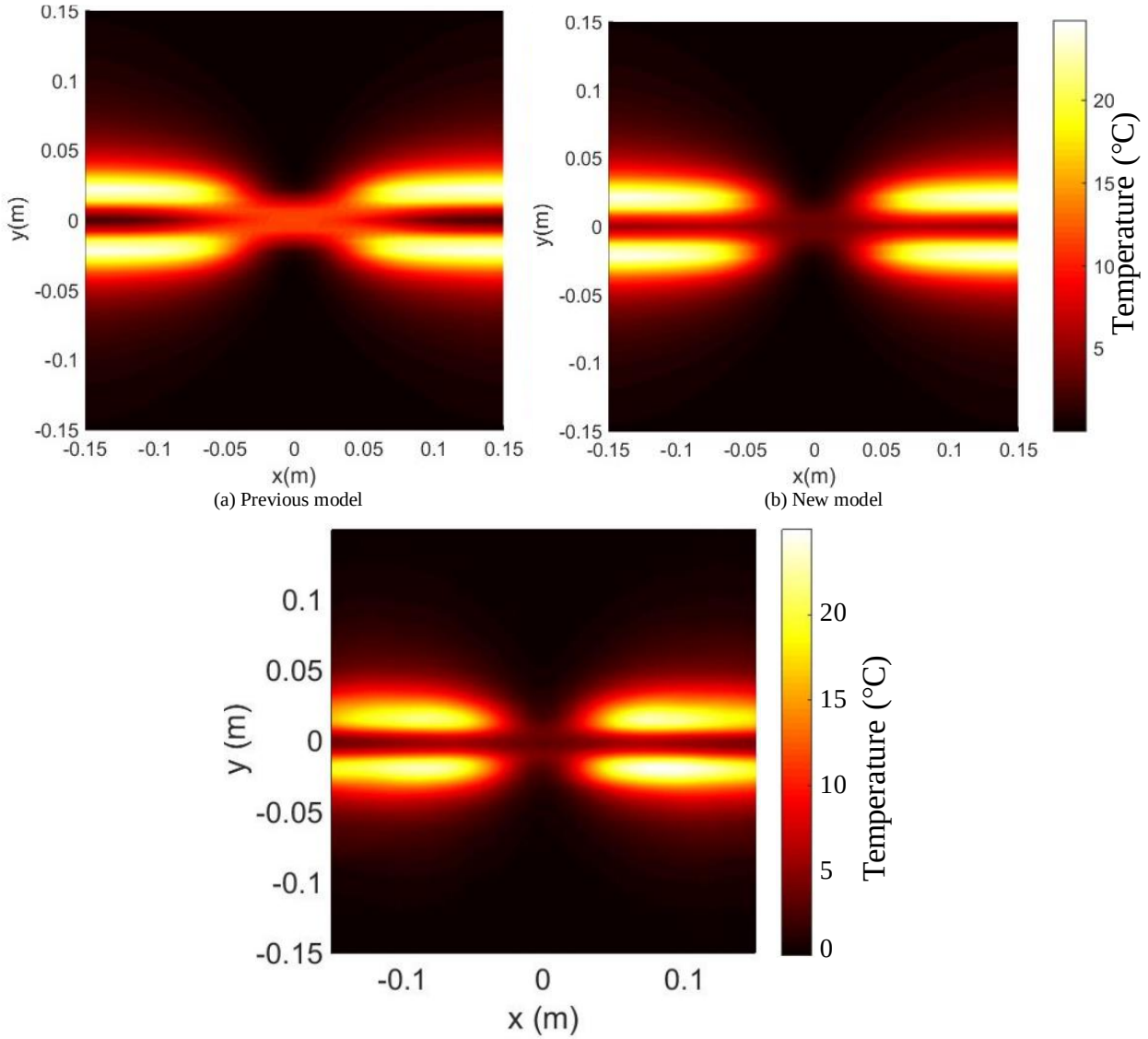

(a) Previous model

(b) New model

(c) Experimental

Fig. 11. Temperature map for 14-ply composite

Source: Authors' own work

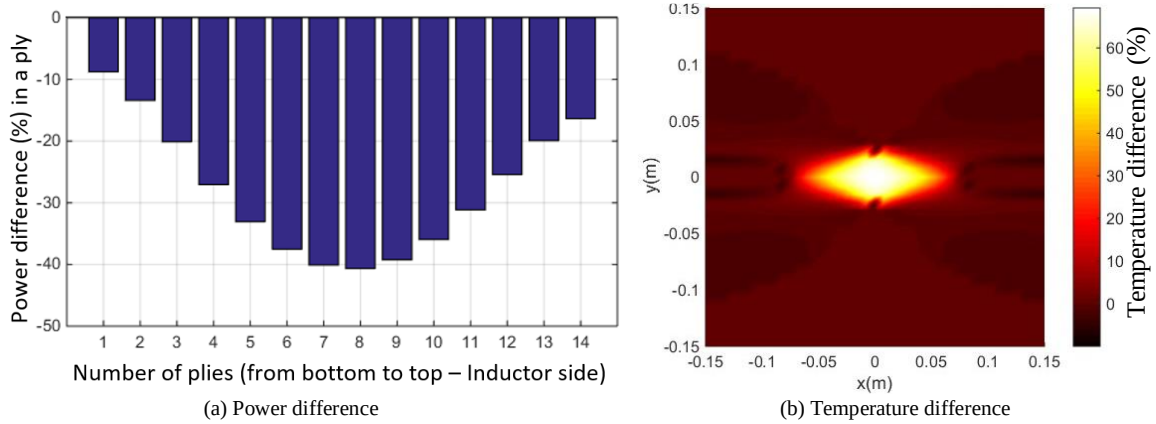

(a) Power difference

(b) Temperature difference

Fig. 12. Difference between new and previous models

Source: Authors' own work

V. Conclusion

In this paper, a novel model of the electrical behavior of stratified composites, incorporating inter-ply interface phenomena revealed by measurements, has been proposed. The model is validated through experimental measurements and a sensitivity study. Furthermore, the new model enables a more accurate estimation of the temperature distribution in CFRP laminate composites.

VI. References

Ahmed, T. J., Stavrov, D., Bersee, H. E. N. & Beukers, A., 2006. Induction welding of thermoplastic composites-an overview. *Composites Part A: Applied Science and Manufacturing*, 37(10), p. 1638–1651.

Buckley JD, F. R., 1988. Rapid Electromagnetic Induction Bonding of Composites, Plastics, & Metals. *MRS Proceedings*, Volume 124, p. 317.

Jaluria, Y. & Torrance, K. E., 2003. *Computational Heat Transfer*. New York: Taylor & Francis.

Kane, B., Pierquin, A., Wasselynck, G. & Trichet, D., 2019. Coupled Numerical and Experimental Identification of Geometrical Parameter for Predicting the Electrical Conductivity of CFRP layers. *IEEE Transactions on Magnetics*, 56(2).

Meltem Altin Karataş, H. G., 2018. A review on machinability of carbon fiber reinforced polymer (CFRP) and glass fiber reinforced polymer (GFRP) composite materials. *Defence Technology*, 14(4), pp. 318-326.

Park, J. B., Hwang, T. K., H. G. Kim & Doh, Y. D., 2007. Experimental and numerical study of the electrical anisotropy in unidirectional carbon-fiber- reinforced polymer composites. *Smart materials and Structures*, Volume 16, p. 57–66.

Qian, Z. et al., 2019. Review on the Electrical Resistance/Conductivity of Carbon Fiber Reinforced Polymer. *Applied Sciences*, 9(11).

Todoroki, A., Tanaka, M. & Shimamura, Y., 2002. Measurement of orthotropic electric conductance of CFRP laminates and analysis of the effect on delamination monitoring with an electric resistance change method. *Composites Science and Technology*, 62(5), p. 619–628.

Wasselynck, G., Trichet, D. & Fouladgar, J., 2013. Determination of the electrical conductivity tensor of a CFRP composite using a 3-D percolation model. *IEEE Transactions on Magnetics*, 49(5), p. 1825–1828.

Wasselynck, G., Trichet, D., Ramdane, B. & Fouldagar, J., 2010. Interaction between electromagnetic field and CFRP materials: A new multiscale homogenization approach. *IEEE Transactions on Magnetics*, 46(8), p. 3277–3280.